ONCOIMMUNOLOGY
2022, VOL. 11, NO. 1, e2117321 (16 pages)
https://doi.org/10.1080/2162402X.2022.2117321

Taylor & Francis
Taylor & Francis Group

ORIGINAL RESEARCH

OPEN ACCESS Check for updates

Targeting DNA damage response components induces enhanced STING-dependent type-I IFN response in ATM deficient cancer cells and drives dendritic cell activation

Marta Lopez-Pelaez[a], Lucy Young[a], Mercedes Vazquez-Chantada[b], Nadine Nelson[a], Steve Durant[a], Robert W. Wilkinson[a], Edmund Poon[a], Miguel Gaspar[a], Viia Valge-Archer[a], Paul Smith[a], and Simon J. Dovedi[a]

[a]Oncology R&D, AstraZeneca, UK; [b]Discovery Sciences, R&D, AstraZeneca, UK

ABSTRACT

The concept of exploiting tumor intrinsic deficiencies in DNA damage repair mechanisms by inhibiting compensatory DNA repair pathways is well established. For example, ATM-deficient cells show increased sensitivity to the ATR inhibitor ceralasertib. DNA damage response (DDR)-deficient cells are also more sensitive to DNA damaging agents like the DNA crosslinker pyrrolobenzodiazepine (PBD) SG-3199. However, additional antitumor benefits from targeting the DDR pathways, which could operate through the activation of the innate immune system are less well studied. DNA accumulation in the cytosol acts as an immunogenic danger signal, inducing the expression of type-I interferon (IFN) stimulated genes (ISGs) by the activation of the cGAS-STING pathway. Here, we demonstrate that ATM $^{-/-}$ FaDu tumor cells have higher basal expression of ISGs when compared to WT cells and respond to ceralasertib and PBD SG-3199 by inducing higher levels of ISGs in a cGAS-STING-dependent manner. We show that sensitive tumor cells treated with ceralasertib and PBD SG-3199 activate dendritic cells (DCs) via a type-I IFN-dependent mechanism. However, STING deficiency in tumor cells does not prevent DC activation, suggesting that transactivation of the STING pathway occurs within DCs. Furthermore, depletion of the cytosolic DNA exonuclease TREX1 in tumor cells increases DC activation in response to PBD SG-3199-treated tumor cells, indicating that an increase in tumor-derived cytosolic DNA may further enhance DC activation. In summary, in this study, we show that ceralasertib and PBD SG-3199 treatment not only intrinsically target tumor cells but also extrinsically increase tumor cell immunogenicity by inducing DC activation, which is enhanced in ATM-deficient cells.

ARTICLE HISTORY
Received: 22 December 2021
Revised: 16 August 2022
Accepted: 16 Aug 2022

Keywords
DNA damage repair; DDR; ATR; ATM; ceralasertib; PBD SG-3199; Interferon; DC; STING; TREX1

Introduction

The treatment of cancer by radiotherapy and chemotherapy agents often relies on the accumulation of DNA damage, ultimately leading to cell death as a function of uncontrolled proliferation coupled with dysfunctional DNA repair mechanisms. DNA damage can be repaired by multiple DNA damage repair pathways; however, the intrinsic impairment of these pathways is common in cancer cells and leads to dependency on compensatory DNA repair mechanisms. Therefore, inhibiting DNA damage responses with targeted therapies can induce tumor cell death by synthetic lethality in specific tumor genotypes[1] and can also be used in combination with DNA damaging agents. This has been shown in the case of Ataxia Telangiectasia and Rad3-related (ATR) and Ataxia Telangiectasia Mutated (ATM) proteins, two apical DNA damage signaling kinases, where ATR inhibition has been reported to induce synthetic lethality in ATM-deficient cells.[2] Also, defects in DNA damage repair sensitize cells to DNA damaging agents such as the pyrrolobenzodiazepine (PBD) SG-3199; a warhead used in antibody drug conjugates (ADC),[3] which binds to the DNA minor groove thereby cross-linking DNA and inducing cytotoxicity.

In addition to the direct antitumor effect that increasing DNA damage with chemo- and radiotherapy has on cancer cells, some cancer therapies such as anthracyclines[4] and radiation[5] not only exert direct antitumor activity but can also have an indirect activity by inducing an antitumor immune response. Treated dying tumor cells can release damage-associated molecular patterns (DAMPs) recognized by dendritic cells (DCs) as a cellular stress trigger via pattern-recognition receptors (PRRs)[6] and can induce the uptake of the dying tumor cells by dendritic cells, a process called efferocytosis,[7] as well as trigger multiple pro-inflammatory responses. Consequently, DCs can process and present tumor antigens to $CD8^+$ T cells in an adequate cytokine context required for the priming of tumor antigen specific $CD8^+$ T cells[8–10] and this process plays an essential role in the efficacy of these therapies.

Cytosolic DNA is a danger signal that can be produced by unrepaired DNA damage and trigger multiple pro-inflammatory responses, including the production of type-I IFN.[11] The DNA sensor cyclicGMP-AMP synthase (cGAS) recognizes cytoplasmic dsDNA in a sequence independent manner and produces the second messenger 2',3'-cyclic GMP-AMP (cGAMP). The endoplasmic reticulum adaptor protein STING (stimulator of interferon genes), also known as TMEM173, recognizes cGAMP and oligomerizes to form tetramers which then act as a scaffold for TBK1 activation. TBK1

CONTACT Simon J. Dovedi Simon.Dovedi@astrazeneca.com Oncology R&D, AstraZeneca, Cambridge, United Kingdom
Supplemental data for this article can be accessed online at https://doi.org/10.1080/2162402X.2022.2117321

then phosphorylates the transcription factors IRF3 and NFκB leading to their homodimerization and nuclear translocation resulting in the induction of type-I IFN expression.[12–16] The activation of STING has been reported to be essential to induce type-I IFN in response to intracellular exogenous DNA from pathogens and more recently to be also involved in the immune response against tumors. It has been reported that the activation of STING in antigen presenting cells (APCs) is required for the activation of antigen specific $CD8^+$ T cells against tumor cells.[17] Moreover, the IFN-driven antitumor activity induced by radiation therapy has been shown to be STING-dependent.[18] Also, direct activation of STING in tumors induces a potent antitumor immunity in mice.[19]

To further understand how targeting the DNA damage response in cancer cells can potentiate an antitumor immune response, we studied the effects of the ATP competitive ATR inhibitor ceralasertib (AZD6738)[20] and the DNA damaging agent PBD SG-3199 on modulating the activation of the immune system and how deficiency in the DDR protein ATM can modulate this process. We have observed that targeting the DNA damage response in cancer cells results in the increased production of ISGs by cancer cells via a STING-dependent mechanism, the efferocytosis of drug-treated sensitive tumor cells and activation of DCs, which was enhanced in ATM-deficient tumor cells. These results demonstrate the direct antitumor effect of ceralasertib and PBD SG-3199 on sensitive cancer cells is compounded by an indirect antitumor effect from the immune system as a result of increased immunogenicity of the drug-treated cancer cells.

Materials and methods

Cell lines and media

All cell lines used in the experiments described in this article were kept in culture for a maximum of 2 months before starting new cultures from master vials. FaDu WT and FaDu ATM $^{-/-}$ cells[21] were obtained from internal stocks and were cultured in MEM (Gibco) supplemented with 10% FBS (Gibco) and 1% NEAA (Gibco). THP-1-dual WT, STING $^{-/-}$ and TREX1 $^{-/-}$ cells were obtained from Invivogen and were cultured in RPMI 1640 Glutamax media (Gibco), supplemented with HEPES (ThermoFisher Scientific), 10% FBS (Gibco), 0.05 mM β-mercaptoethanol (ThermoFisher Scientific) and the selection antibiotics blasticidin (10 µg/ml) and zeocin (10 µg/ml) (both Invivogen). The selection antibiotics were removed from the culture media to perform the experiments. All cell lines were verified in-house by short tandem repeat (STR) fingerprinting and routinely tested for mycoplasma.

DNA damage induction, inhibitors and agonists

DNA damage was induced by ionizing radiation (IR) with the indicated Gray (Gy) in the figure legends using a Faxitron CellRad irradiator (130 kV, 5 mA, 0.5 mm Al) or by treatment of cells with PBD SG-3199 (40 pM for FaDu cells and 400 pM for THP-1 cells)[3] obtained from internal stock. Ceralasertib [20] (1 µM) or AZD0156 [22] (10 nM) were obtained from internal stocks, recombinant human IFNβ (300 U/ml, R&D) and the JAK1/2 inhibitor INCB018424 ruxolitinib (1 µM, Chemietek) were obtained commercially. The cGAS agonist dsDNA HT-DNA (25 µg/ml, Sigma) and the STING agonist 2′3′-cGAMP (25 µg/ml, Invivogen) were transfected into tumor cells using 2 µl Lipofectamine™ 2000 (ThermoFisher Scientific) according to manufacturer's instructions.

Cell cycle, proliferation, apoptosis, cell death and micronuclei formation assays

For cell cycle analysis assays, cells were fixed with 70% ethanol at −20°C for at least 16 hours followed by washing with PBS and staining with propidium iodide solution containing RNase (FxCycle™ PI/RNase, Life technologies) as per the manufacturer's instructions and analyzed by flow cytometry. For proliferation assays, percentage of cell confluency was determined by analyzing phase contrast images acquired every two hours for five days in the Incucyte ZOOM System (Sartorius). Alternatively, cells were incubated with CellTiter-Glo reagent (Promega) following manufacturer's instructions and luminescence was measured on the EnVision instrument. For apoptosis and cell death assays, cells were stained with Dead Cell Apoptosis Kit with Annexin V Alexa Fluor™ 488 & Propidium Iodide (PI) (Invitrogen) as per the manufacturer's instructions and analyzed by flow cytometry. Early apoptotic cells (defined as percentage of $AnnexinV^+PI^-$) and dead cells (defined as percentage of $AnnexinV^+PI^+$ cells) of the single cell population were quantified using FlowJo. Alternatively, cells were stained with Live/Dead Fixable Blue Dead Cell Stain (ThermoFisher Scientific) for 30 minutes and percentage of dead cells was defined as percentage of $blue^+$ cells within the single cell population. For micronuclei formation assay, FaDu cells ($1e^4$) were plated in cell carrier-96 ultra-well plates (Perkin Elmer). Following treatments, cells were fixed with 4% formaldehyde in PBS and stained with Hoechst (10 µg/ml) and HCS CellMask Deep Red stain (1 µg/ml) (both Invitrogen) in 0.1% Triton X – 100 (Sigma) in PBS for 30 minutes at room temperature in the dark. Images were acquired with a Yokogawa CV7000 confocal scanner (40x objective) and analyzed using Columbus software (Perkin Elmer) as described in.[23]

siRNA knockdown and RT-qPCR

Cells ($2e^5$) were transfected with siRNA-lipofectamine RNAiMAX complexes (30 pM siRNA/ 1 µl lipofectamine™ RNAiMAX) as per the manufacturer's instructions (Thermo Fisher Scientific). siRNA encoding STING (ID: s50644), cGAS (ID: s41746) and Cy3-labeled negative control were from Ambion (Life Technologies). Total RNA extracted using RNeasy Plus Mini Kit (50) (QIAGEN) and reverse transcribed using high-capacity cDNA reverse transcription kit (Applied Biosystems). Then, cDNA was incubated with the indicated TaqMan gene expression probes (FAM) (Ifnb1 Hs01077958_s1, Isg15 Hs00192713_m1, Ifit1 Hs00356631_g1, Ifi16 Hs00194261_m1, Mx1 Hs00895608_m1, Cxcl10/ IP-10 Hs00171042_m1), Human GAPDH Endogenous Control (VIC) (4326317E) and TaqMan™ Fast Advanced Master Mix (4444557) (all Thermo Fisher Scientific). The cDNA

corresponding to the amplified mRNA was quantified using the ΔΔ cycle threshold (CT) method normalizing to GAPDH.

Western blot

Cells were detached with Accutase (Sigma), collected and lysed in RIPA buffer (Pierce) supplemented with complete phosphatase and protease inhibitors (Cell signaling). Proteins were quantified by BCA (ThermoFisher Scientific) and 20 µg of proteins were separated by gel electrophoresis in NuPAGE 4–12% Bis-Tris Gel Novex (ThermoFisher Scientific) with NuPAGE 1x MOPS buffer (Life technologies). Proteins were transferred to nitrocellulose membrane (Life technologies) by iBlot™ 2 Transfer Device (ThermoFisher Scientific). Membranes were blocked with Odyssey blocking buffer PBS (LI-COR) and probed with primary antibodies as indicated for 16 hours at 4°C at a concentration of 1:500 for Phospho-histone H2A.X (Ser139) (Cell Signaling 2577), Phospho-P-53 (Ser 15) (Cell Signaling 9284), Phospho-STAT1 (Tyr701) (58D6) (Cell Signaling 9167), STING (D2P2F) (Cell Signaling 13647) and cGAS (D1D3G) (Cell Signaling 15102), P-S1981-ATM [EP1890Y] (Abcam 81292) and GAPDH (Millipore MAB374), followed by either IRDye680LT goat anti-rabbit (LI-COR, 926–68021) or IRDye800CW goat anti-mouse (LI-COR, 925–32210) as per the manufacturer's instructions and analyzed in LI-COR Odyssey.

Cytokine analysis

IFNβ and IP-10 concentrations in the culture media were measured by meso-scale discovery (MSD) assay using the human U-plex kit following manufacturer's instructions.

Human monocyte-derived dendritic cell generation and co-culture with treated tumor cells

Human PBMCs (peripheral blood mononuclear cells) were isolated from leukocyte cones from healthy volunteers with Ficoll-Paque PLUS (GE Healthcare). Monocytes ($CD14^+$) were isolated from PBMCs using EasySep™ Human CD14 Positive Selection Kit II (Stemcell) and differentiated to DCs with IL-4 (100 ng/ml, Peprotech) and GM-CSF (100 ng/ml, Peprotech) in RPMI 1640 medium Glutamax ™ -I (Gibco) supplemented with 10% FBS and penicillin/streptomycin (Gibco) for 6 days. At day 3 of differentiation, fresh IL-4 (100 ng/ml) and GM-CSF (100 ng/ml) were added to the media. Tumor cell lines were labeled with CellTrace violet (Invitrogen) as per the manufacturer's instructions and plated. The following day, the tumor cells were treated with compounds for 48 hours or with ionizing radiation for 24 hours as indicated in the figures. Then, the tumor cells were collected by accutase treatment, washed twice with PBS and counted. $2e^5$ tumor cells were co-cultured with $1e^4$ dendritic cells for 24 hours (ratio 20:1 target tumor cell: effector dendritic cell). Alternatively, $1e^4$ dendritic cells were stimulated with 10 ng/ml LPS (O26:B6) from Sigma (L2654, lot 025M4088) for 24 hours as positive control or treated with compounds for 48 hours. Cells were then collected, washed with PBS, stained with Live/Dead Fixable Blue Dead Cell Stain (ThermoFisher Scientific) for 30 minutes followed by staining with CD11c-PerCP (Clone Bu15, Biologend 337234), CD86-PE (Clone IT2.2, BD 555665), CD80-FITC (Clone L307.4, BD 557226), and HLA-DR-APC/Cyanine7 (Clone L243, Biolegend 307618) in flow cytometry staining buffer (eBioscience), cells were analyzed in a BD Fortessa cytometer and data was analyzed with FlowJo. Efferocytosis was defined as percentage of $CD11c^+$ CellTrace $Violet^+$ cells within live $CD11c^+$ single cell population, and DC activation was measured as mean fluorescence intensity (MFI) of CD86, CD80 or HLA-DR (within the $CD86^+CD11c^+$, $CD80^+CD11c^+$ or $HLA\text{-}DR^+CD11c^+$ live single cell populations, respectively). DC viability was determined as percentage of live cells (blue $dead^-$ $CD11c^+$ cells within single cell population.

Results

ATM-deficient tumor cells are more sensitive to treatment with the ATR inhibitor ceralasertib or DNA damage induction by PBD SG-3199

Tumor cells with defects in the DNA damage response pathway have been shown to be more susceptible to DNA damage induction[3] and ATR inhibition has been described to induce synthetic lethality in ATM $^{-/-}$ cells.[2,20,24] To confirm these results, we treated FaDu ATM $^{-/-}$ cells with the ATR inhibitor ceralasertib or with the DNA damaging agent PBD SG-3199 and analyzed the effect on cell cycle progression and cell death. Treatment with ceralasertib[20] induced phosphorylation of the DNA damage marker γ-H2AX in both FaDu WT and FaDu ATM $^{-/-}$ tumor cells, whereas it induced phosphorylation of the downstream protein p53 only in WT cells, consistent with requiring ATM activity for phosphorylation (Figure 1a). ATM $^{-/-}$ cells had a lower percentage of cells in G1 (Figure 1b **and S1A)** as well as an increased early apoptosis by 48 hours and cell death by 72 hours of culture in DMSO treated controls in comparison with WT cells (Figure 1c). Moreover, ceralasertib induced an increase in the S-phase fraction in WT cells after 48 hours of treatment whereas in ATM $^{-/-}$ cells occurred by 24 hours, and was enhanced in comparison with WT cells (Figures 1b **and S1A)**. Ceralasertib also increased the G2/M fraction of cells by 72 hours in ATM $^{-/-}$ cells but not in WT cells (Figure 1b **and S1A)**. Furthermore, ceralasertib induced early apoptosis (Figure 1b–c **and S1A)** and cell death (Figure 1c) and inhibited proliferation **(Figure S1B)** in ATM $^{-/-}$ cells but not in WT cells.

Treatment with PBD SG-3199 induced the phosphorylation of γ-H2AX and p53, cell cycle arrest in both S and G2/M phases, inhibition of proliferation, early apoptosis, and cell death in both WT and ATM $^{-/-}$ FaDu cancer cells (Figures 1a–c **and S1A–B)**. However, WT cells had enhanced cell cycle arrest in response to PBD SG-3199 compared with ATM $^{-/-}$ cells (Figures 1b **and S1A)**, whereas ATM $^{-/-}$ cells had increased inhibition of proliferation **(Figure S1B)**, early apoptosis (Figures 1b–c **and S1A)**, and tumor cell death (Figure 1c) compared with WT tumor cells. In conclusion, ATM $^{-/-}$ tumor cells are more sensitive to ATR inhibition and to DNA damage.

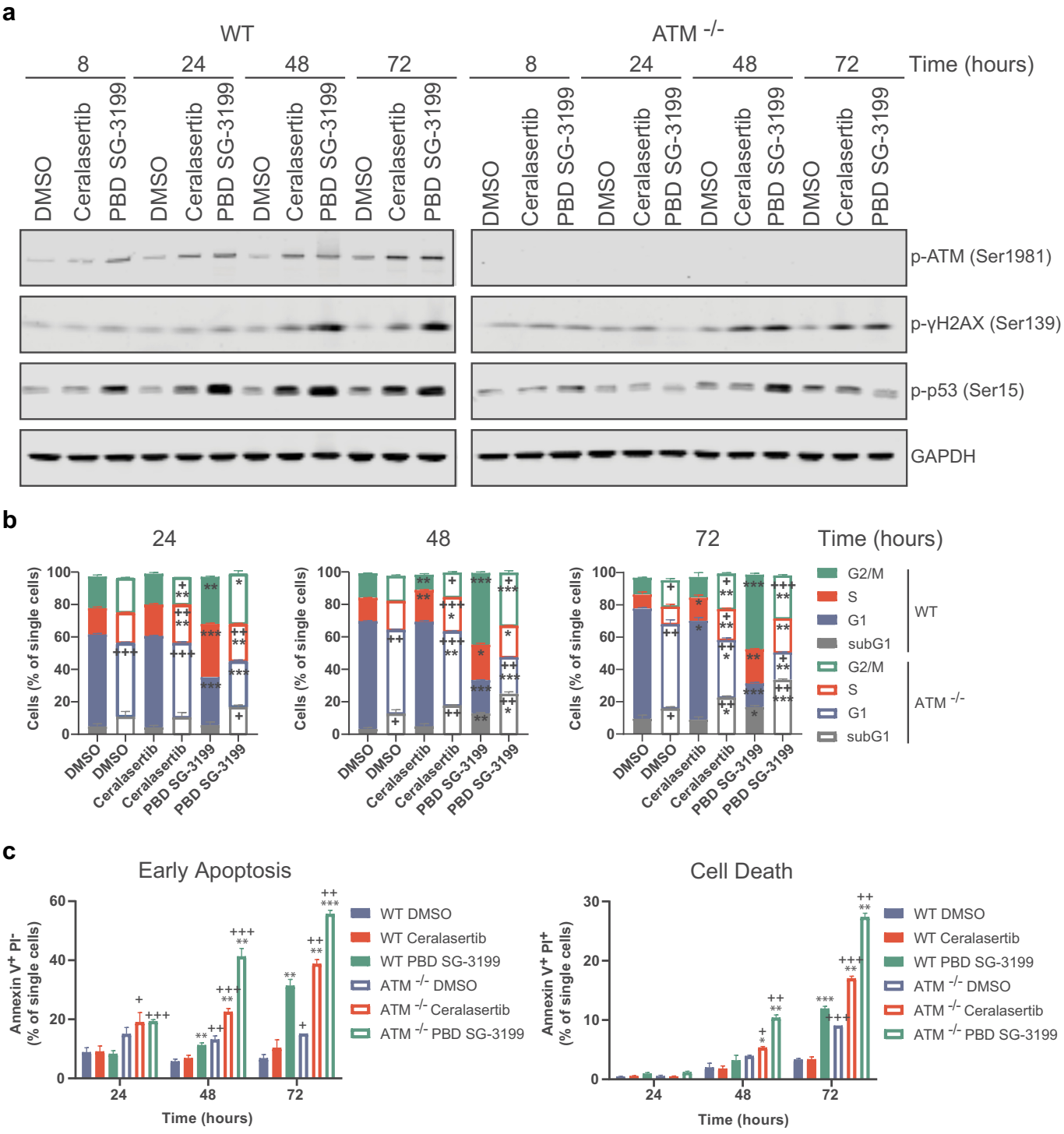

Figure 1. Enhanced sensitivity of ATM-deficient tumor cells to ATR inhibition and DNA damage.
FaDu WT and FaDu ATM $^{-/-}$ cells were treated with ceralasertib (1 μM), PBD SG-3199 (40 pM) or DMSO for the times indicated. (a) Cell lysates were subjected to SDS/PAGE and immunoblotted with antibodies to the indicated proteins. (b) Cell cycle analysis by flow cytometry. Data are shown as mean + SEM percentage of cells in subG1/apoptotic, G1, S and G2/M stages of the cell cycle of the single cell population from three independent experiments. Each experiment was performed in duplicate. (c) Apoptosis and cell death analysis by flow cytometry. Data are shown as mean + SEM of percentage of early apoptotic cells (AnnexinV^{+}PI^{-}) and dead cells (AnnexinV^{+}PI^{+}) of the single cell population from two independent experiments. Each experiment was performed in duplicate. (b-c) Statistical testing by t-test ($p < .05$ *, $p < .01$ **, $p < .001$ *** comparing treatment vs DMSO control in each genotype; t test $p < .05$ +, $p < .01$ ++, $p < .001$ +++ comparing each treatment group in WT vs ATM $^{-/-}$ cells). See also Supplementary Figure S1.

ATR inhibition or treatment with PBD SG-3199 leads to enhanced micronuclei formation in ATM-deficient cells

It has been proposed that double-stranded DNA breaks generated by ionizing radiation (IR) leads to the formation of micronuclei during cell cycle progression through mitosis[25,26] and ATR inhibition has been previously shown to induce micronuclei formation[23,27] and this is enhanced in ATM $^{-/-}$ cells.[23] Therefore, we investigated if PBD SG-3199 can also induce micronuclei formation and if this is increased by

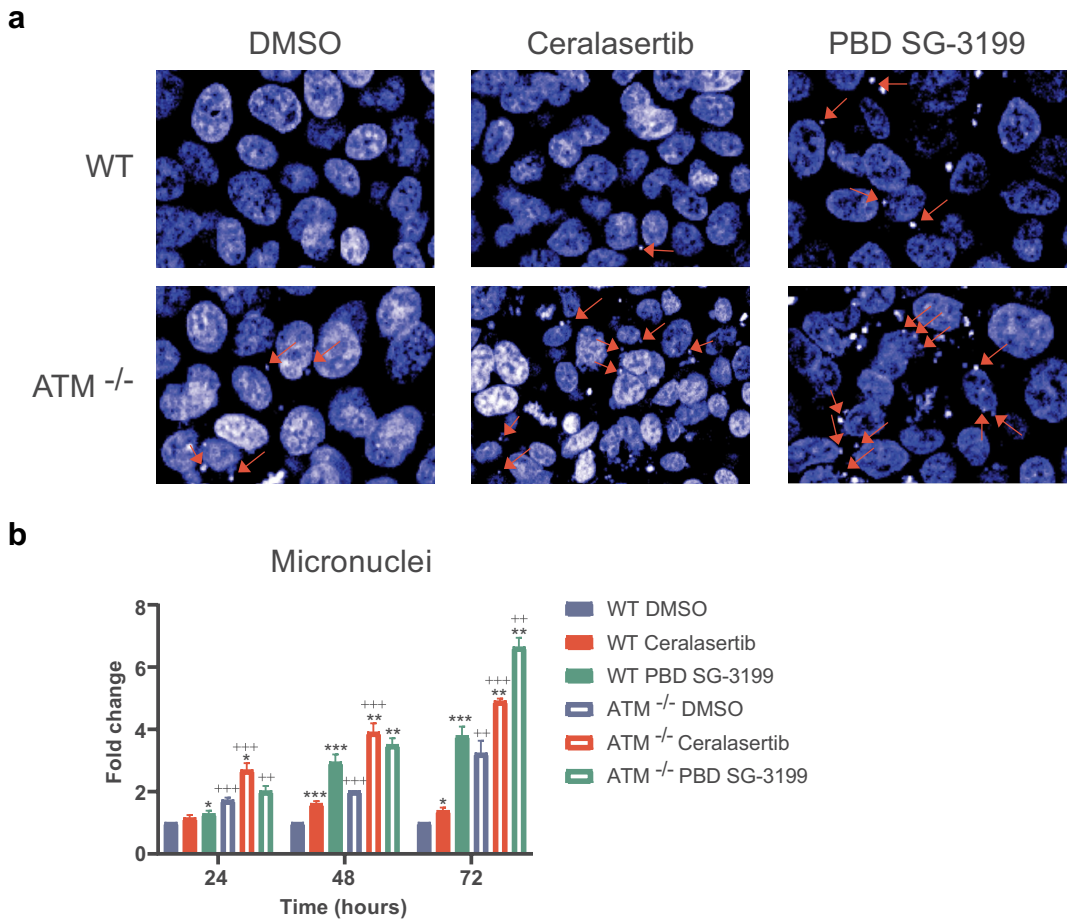

Figure 2. ATR inhibition and PBD SG-3199 induce increased micronuclei formation in ATM-deficient cells.
FaDu WT and FaDu ATM $^{-/-}$ cells were treated with ceralasertib (1 μM), PBD SG-3199 (40 pM) or DMSO as control for the times indicated and analyzed by automated microscopy for micronuclei formation. (a) Representative images after 72 hours of treatment. Red arrows indicate micronuclei. (b) Quantification of micronuclei. Data shown as mean + SEM fold increase of micronuclei per number of nucleus compared with WT cells treated with DMSO at each end point from three independent experiments. Each experiment was performed in duplicate or triplicate. Statistical testing by t-test ($p < .05$ *, $p < .01$ **, $p < .001$ *** comparing treatment vs DMSO control in each genotype; $p < .05$ +, $p < .01$ ++, $p < .001$ +++ comparing each treatment group in WT vs ATM $^{-/-}$ cells).

ATM deficiency in tumor cells. Treatment of both WT and ATM $^{-/-}$ tumor cells with either ceralasertib or PBD SG-3199 induced the formation of micronuclei (Figure 2a–b **and S2)**. ATM depletion induced enhanced micronuclei formation in response to ceralasertib (Figure 2a–b **and S2**) and PBD SG-3199 (Figure 2a–b). Furthermore, ATM $^{-/-}$ tumor cells had higher basal levels of micronuclei[23] (Figure 2a–b). Of note, the fold increase of micronuclei above DMSO control in response to PBD SG-3199 was reduced in ATM $^{-/-}$ cells in comparison to WT cells **(Figure S2)**, probably due to already high basal levels of micronuclei (Figure 1a–b) and/or increased levels of cell death in ATM $^{-/-}$ cells (Figure 1b–c **and S1A)**. These results confirm the published findings on ceralasertib and show that increasing DNA damage with PBD SG-3199 also results in micronuclei formation and that this is enhanced in ATM $^{-/-}$ cells.

ATR inhibition and DNA damage induce a type-I IFN response which is increased in ATM-deficient cells

We have shown that ceralasertib and PBD SG-3199 induce higher levels of DNA damage and cell death in ATM $^{-/-}$ tumor cells compared to WT counterparts. Some cancer therapies can also exert an indirect antitumor effect by inducing the activation of the immune system via the release of danger signals such as type-I IFN.[28] It has been proposed that DNA damage can induce the production of type-I IFN through the activation of the STING pathway by cytosolic DNA.[29] Moreover, micronuclei can be recognized by cGAS leading to STAT1 activation and type-I IFN production.[26] The extrinsic effect that ceralasertib and PBD SG-3199 can exert on the activation of the immune system has not been characterized. Therefore, we explored the induction of type-I IFN production in response to ceralasertib and PBD SG-3199 in tumor cells deficient or proficient for ATM. Firstly, as some cancer cells have a deficiency in the activation of the STING pathway which is associated with poor prognosis,[30,31] we validated our model system to confirm competency for STING and type-I IFN activation. To this aim, we studied the mRNA induction of type-I IFN genes in response to transfection with the specific STING agonists dsDNA HT-DNA and 2′3′-cGAMP[32,33] **(Figure S3A)** and to stimulation with IFNβ. In response to dsDNA and IFNβ, there was significant mRNA induction of all the ISG studied (IFNβ, IP-10, ISG15, MX1, IFI16 and IFIT1) in

FaDu WT and ATM $^{-/-}$ cells **(Figure S3B–G)**. 2′3’-cGAMP treatment in ATM $^{-/-}$ tumor cells also induced mRNA expression of all the ISG genes studied, however it significantly induced only ISG15, MX1 and IFI16, but not IFNβ, IP-10 or IFIT1 in WT tumor cells **(Figure S3B–G)**. Moreover, we observed mRNA induction of all ISGs in response to HT-DNA, 2′3’-cGAMP and IFNβ was significantly enhanced in ATM $^{-/-}$ cells **(Figure S3B–G)**. These data corroborate that human FaDu tumor cells have a proficient STING-IFN pathway, and that ATM deficiency enhances sensitivity to STING agonists and IFNβ stimulation.

We then investigated the effect of ceralasertib and PBD SG-3199 on the mRNA induction of a type-I IFN mRNA signature in WT and ATM $^{-/-}$ cells. Treatment with either ceralasertib or PBD SG-3199 induced the mRNA expression of IFNβ and type-I IFN stimulated genes (Figure 3a-f **and S4A–F)**. Moreover, we observed that ATM $^{-/-}$ FaDu tumor cells had higher basal level of ISGs transcripts (Figure 3a–f **and S3B–G)** and an enhanced induction of ISG transcripts in response to ceralasertib (Figure 3a–f **and S4A–F)**. PBD SG-3199 also induced a more rapid increase of ISG transcripts in ATM $^{-/-}$ cells as observed at 24 hours (Figure 3a–f **and S4A–F)**. However, for some ISGs, mRNA induction was significantly higher at 48 hours in WT cells (Figure 3a–f) and the fold change of ISG mRNAs above DMSO control in response to PBD SG-3199 was reduced in ATM-deficient cells in comparison to WT cells at 48 hours **(Figure S4A–F)**, possibly accounted for by increased apoptosis and cell death in ATM $^{-/-}$ cells as shown in Figure 1b–c and **S1A**. Moreover, cytokine release of IFNβ and the ISG IP-10 was also increased in ATM $^{-/-}$ cells treated with ceralasertib and PBD SG-3199, as well as in basal conditions, in comparison with WT cells (Figure 3g–h). Furthermore, inhibition of ATM with the ATM inhibitor AZD0156[34] in WT cells treated with ceralasertib or PBD SG-3199 led to increased mRNA expression of IFNβ compared with ATM inhibition alone **(Figure S5A–B)**. However, treatment of WT tumor cells with AZD0156 **(Figure S5A–B)** failed to reproduce the increased basal mRNA expression of IFNβ observed in the ATM $^{-/-}$ tumor cells (Figure 3a **and S3B)**, suggesting differences in phenotype between complete loss of ATM and pharmacological inhibition. A potential caveat to these data is that the Fadu ATM $^{-/-}$ lineage may have deviated from the parental cells as a consequence of gene silencing and clonal selection. Taken together, these data indicate that ATR inhibition and induction of DNA damage by PBD SG-3199 induce the expression of ISGs and that this induction is enhanced by ATM deficiency or ATM inhibition.

Induction of IFNβ following ATR inhibition or DNA damage is dependent on signaling through cGAS-STING

The induction of type-I IFN by DNA damage has been proposed to occur by the activation of the cGAS-STING pathway.-[35] Since ceralasertib and PBD SG-3199 induce the expression of type-I ISGs, we investigated if this was dependent on the activation of the cGAS-STING pathway. Depleting cGAS or STING in FaDu cells by siRNA (Figure 4a) abolished the induction of IFNβ mRNA by ceralasertib and PBD SG-3199 in both FaDu WT and FaDu ATM $^{-/-}$ cells (Figure 4b **and S6)** showing that activation of the cGAS-STING pathway in these tumor cells is required. Moreover, PBD SG-3199 also induced IFNβ mRNA in THP-1 tumor cells and this induction was greatly reduced by STING depletion (Figure 4c), demonstrating that IFNβ induction by PBD SG-3199 in THP-1 tumor cells is also STING dependent.

ATM-deficient tumor cells treated with ATR inhibitor or DNA damaging agents induce enhanced efferocytosis and DC activation

It has been reported that radiation induces STING activation, and this may be required for DC activation and cross-priming.[18] Here, we have shown that ceralasertib and PBD SG-3199 induce STING-dependent type-I IFN signaling. To investigate if ceralasertib and PBD SG-3199 treatment of tumor cells modulates the response of DCs against these tumor cells, we co-cultured DCs with CellTrace violet-labeled drug-treated tumor cells, then analyzed the uptake of dying drug-treated tumor cells and debris by DCs, a process known as efferocytosis,[7] and determined DC activation by measuring the induction of the co-stimulatory molecules CD86 and CD80, and the MHC-II molecule HLA-DR[36,37] by flow cytometry **(assay schematic in** Figure 5a). Pre-treatment of ATM $^{-/-}$ but not WT FaDu cells with ceralasertib induced an increase in efferocytosis (Figure 5b) and DC activation as detected by increase in the MFI of the activation markers CD80, CD86 and HLA-DR (Figure 5c–e). The co-culture of PBD SG-3199 treated FaDu cells with DCs induced efferocytosis and dendritic cell activation by both WT and ATM $^{-/-}$ cells, but was enhanced in ATM $^{-/-}$ cells (Figure 5b–e). The basal level of efferocytosis and DC activation was increased by ATM deficiency (Figure 5b–e **and S7B-C)**. These data indicate that ATM-deficient tumor cells treated with ceralasertib and PBD SG-3199 induce higher levels of efferocytosis and DC activation than ATM WT tumor cells, consistent with the observed levels of DNA damage and IFNβ mRNA induced by ceralasertib and PBD SG-3199 in the FaDu WT and FaDu ATM $^{-/-}$ tumor cells described above. The TLR4 agonist LPS, used as a positive control in the assay, also induced DC activation (Figure 5c–e). The treatment of DC with either ceralasertib or PBD SG-3199 had no effect on DC viability (Figure 5f). In addition, ATM $^{-/-}$ tumor cells were more sensitive than WT cells to irradiation treatments as shown by the induction of IFNβ in ATM $^{-/-}$ cells at a lower irradiation dose (1 Gy at 48 hours) and the enhanced induction of IFNβ mRNA in ATM $^{-/-}$ vs WT tumor cells **(Figure S7A)**. Irradiated FaDu tumor cells in co-culture with DCs induced efferocytosis of the treated tumor cells and DC activation (**Figure S7B–C**). Similar to ceralasertib or PBD SG-3199 treatments, the treatment of tumor cells with 20 Gy radiation induced enhanced efferocytosis and dendritic cell activation in ATM $^{-/-}$ tumor cells compared to WT (**Figure S7B–C**). Overall, these data indicate that treatment of tumor cells with ceralasertib, or with the DNA-damaging agents IR and PBD SG-3199, induces efferocytosis of sensitive treated tumor cells by DCs and DC activation and this is enhanced in ATM $^{-/-}$ tumor cells.

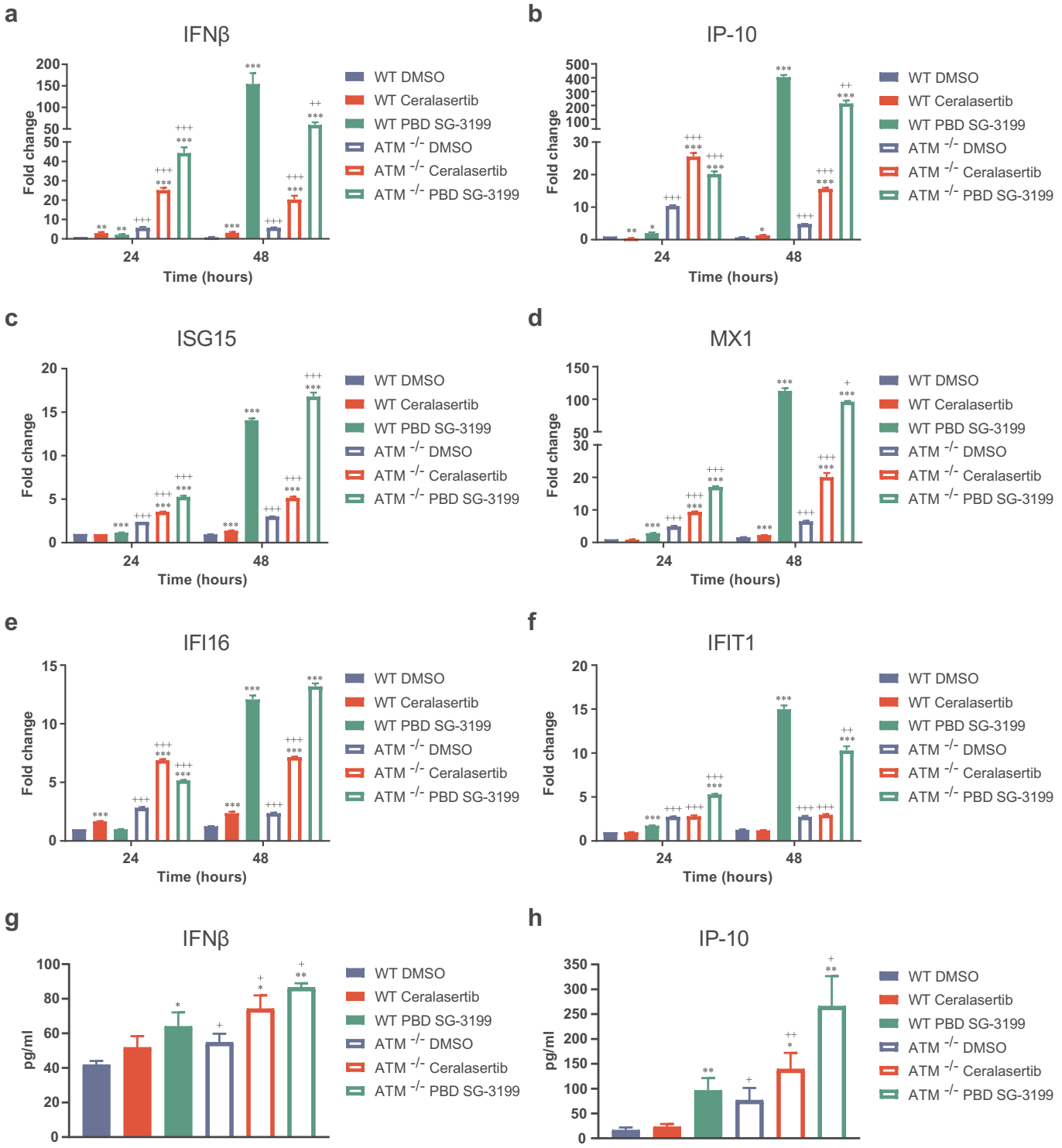

Figure 3. ATR inhibition and DNA damage induce type-I IFN response in FaDu tumor cells which is enhanced in ATM-deficient cells.
(a-f) FaDu WT and FaDu ATM $^{-/-}$ cells were treated with ceralasertib (1 μM), PBD SG-3199 (40 pM) or DMSO for the indicated times. RT-qPCR analysis of the indicated genes. Data normalized to GAPDH shown as mean + SEM fold increase relative to FaDu WT DMSO-treated cells at 24hours from one representative experiment out of two performed. Each experiment was performed in triplicate. (g-h) FaDu WT and FaDu ATM $^{-/-}$ cells were treated with ceralasertib (1 μM), PBD SG-3199 (40 pM) or DMSO for 48 hours. IFNβ and IP-10 (pg/ml) secreted into the culture medium was measured by MSD. Data shown as mean + SEM from three independent experiments. Each experiment was performed in duplicate. (a-h) Statistical testing by t-test ($p < .05$ *, $p < .01$ **, $p < .001$ *** comparing treatment vs DMSO control in each genotype; $p < .05$ +, $p < .01$ ++, $p < .001$ +++ comparing each treatment group in WT vs ATM $^{-/-}$ cells). See also Supplementary Figures S3 and S5.

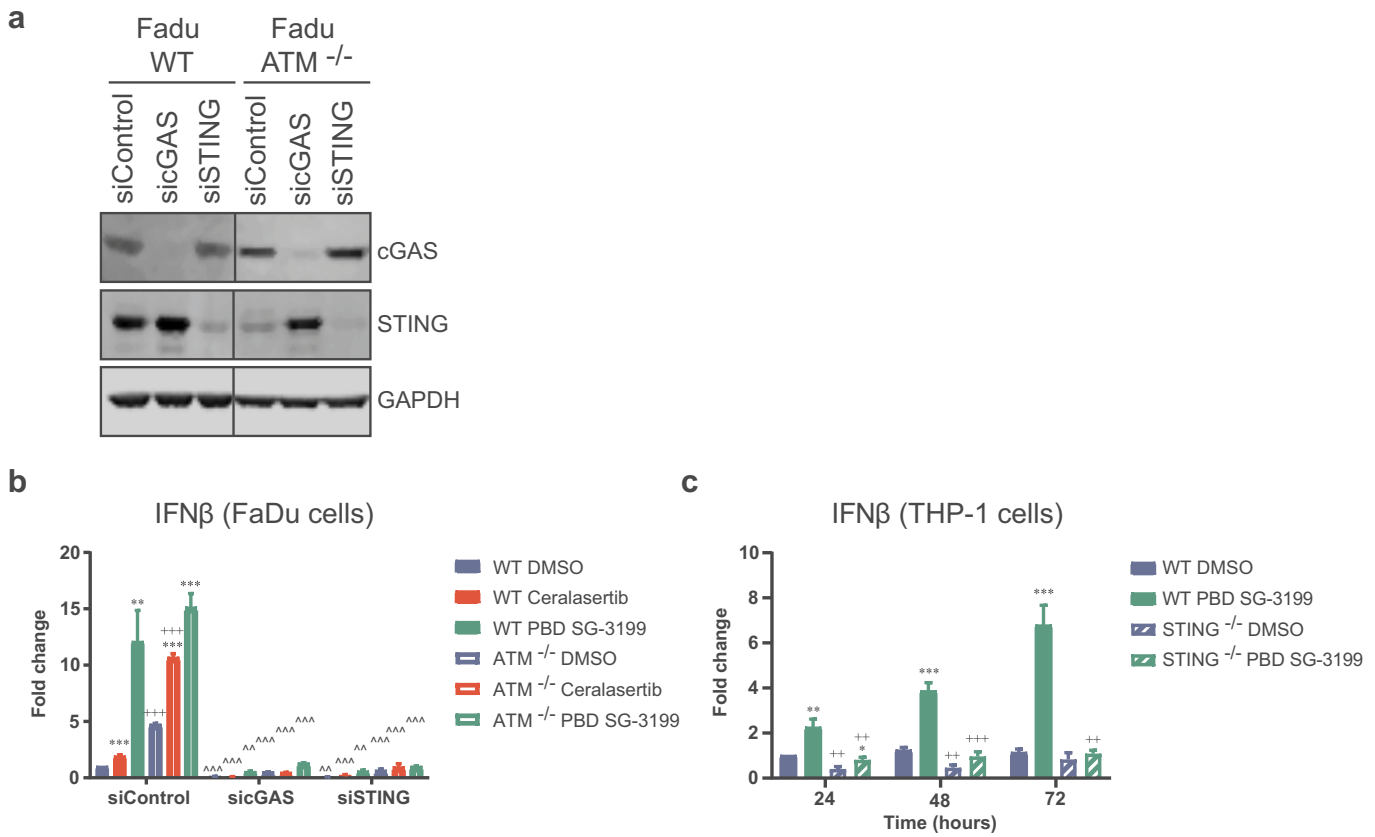

Figure 4. Induction of IFNβ by ATR inhibition or PBD SG-3199 depends on signaling through cGAS and STING.
(a) cGAS- or STING siRNA-mediated downregulation in FaDu WT and FaDu ATM $^{-/-}$ cells analyzed after 72 hours by immunoblot using antibodies against the proteins indicated in the figure. (b) RT-qPCR analysis of IFNβ mRNA expression in FaDu WT and FaDu ATM $^{-/-}$ cells treated with siRNA against cGAS or STING or control for 24 hours followed by treatment with ceralasertib (1 μM) or PBD SG-3199 (40 pM) for 48 hours. Data normalized to GAPDH shown as mean + SEM fold increase relative to FaDu WT DMSO-treated cells from two independent experiments. Each experiment was performed in triplicate. Statistical testing by t-test ($p < .05$ *, $p < .01$ **, $p < .001$ *** comparing treatment vs DMSO control in each genotype in siControl-treated cells; $p < .05$ +, $p < .01$ ++, $p < .001$ +++ comparing each treatment group in WT vs ATM $^{-/-}$ cells in siControl-treated cells; $p < .05$ ^, $p < .01$ ^^, $p < .001$ ^^^ comparing sicGAS or siSTING with siControl in each treatment group and genotype group). (c) RT-qPCR analysis of IFNβ mRNA expression in THP-1 WT and THP-1 STING $^{-/-}$ cells treated with PBD SG-3199 (400 pM) for the times indicated. Data normalized to GAPDH shown as mean + SEM fold increase relative to THP-1 WT DMSO-treated cells from two independent experiments. Each experiment was performed in triplicate. Statistical testing by t-test ($p < .05$ *, $p < .01$ **, $p < .001$ *** comparing treatment vs DMSO control in each genotype; $p < .05$ + , $p < .01$ ++, $p < .001$ +++ comparing each treatment group in WT vs STING $^{-/-}$ cells).

Canonical JAK-STAT signaling is required for DC activation in response to ATR inhibition or DNA damage in tumor cells

Previous studies demonstrate that IFNβ production by DCs in response to irradiated tumor cells is cGAS-STING-IRF3 dependent and is necessary for cross-priming tumor reactive CD8$^+$ T cells.[18,38] Here, we have shown that treatment of tumor cells with ceralasertib and with PBD SG-3199 induced a STING-dependent type-I IFN signature and the activation of DCs in response to the treated tumor cells. IFNβ signals through the type-I interferon receptor activating the JAK-STAT pathway.[39] To investigate if type-I IFN signaling is required for the activation of DCs by tumor cells treated with ceralasertib or with PBD SG-3199, we co-cultured DCs with ceralasertib and PBD SG-3199 treated tumor cells in the presence or absence of the specific JAK1/2 inhibitor INCB018424 (ruxolitinib)[40] (Figure 6a). The results demonstrate that whilst JAK1/2 inhibition does not modulate efferocytosis of ceralasertib or PBD SG-3199 treated tumor cells tumor by DCs (Figure 6b), it does inhibit DC activation (Figure 6c–e). Moreover, ruxolitinib also reduces CD86 and CD80,[41] but not significantly HLA-DR upregulation in response to activation by the positive control LPS (Figure 6c–e). These results demonstrate that DC activation in response to ceralasertib or PBD SG-3199-treated tumors requires canonical JAK-STAT signaling.

DNA damage in TREX1-deficient tumor cells potentiates DC activation

We have shown here that treating sensitive tumor cells with ceralasertib or PBD SG-3199 results in the induction of type-I IFN by the cGAS-STING pathway, efferocytosis and activation of DCs. To further understand if the accumulation of cytosolic DNA in the treated tumor cells is responsible for the observed DC activation, we investigated the role of TREX1, an exonuclease that degrades cytoplasmic DNA and thereby limits activation of STING.[42] In mouse models, TREX1 regulates the activation of the immune system in response to radiation.[43] We analyzed if TREX1 deficiency in tumor cells enhances type-I IFN induction and modulates the activation of DCs in response to DNA damage in the tumor cells. To achieve this,

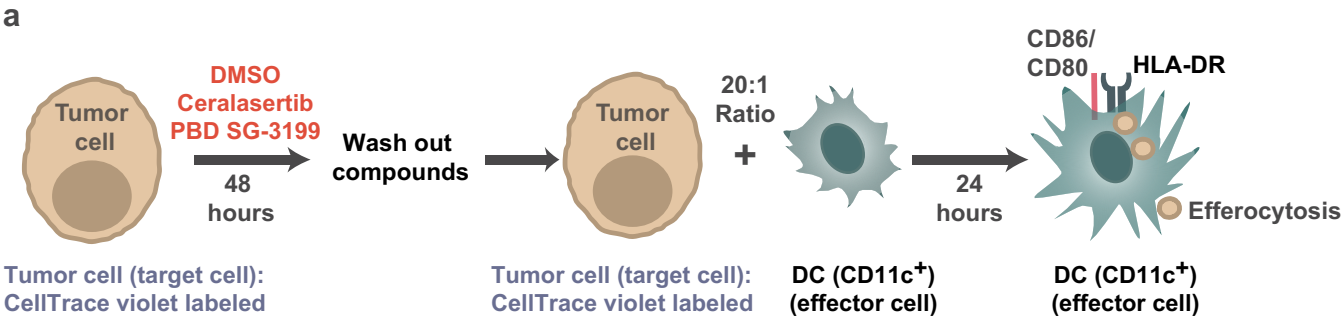

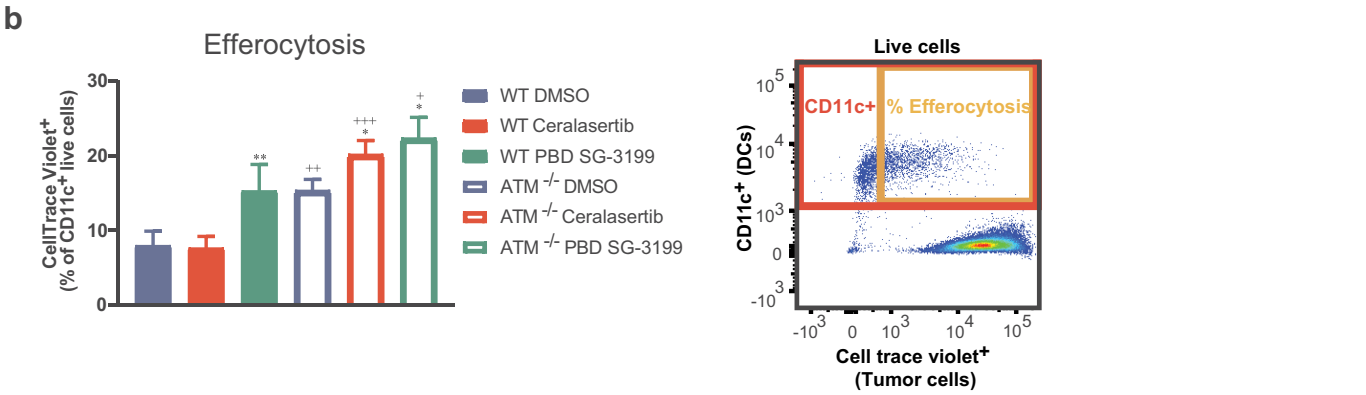

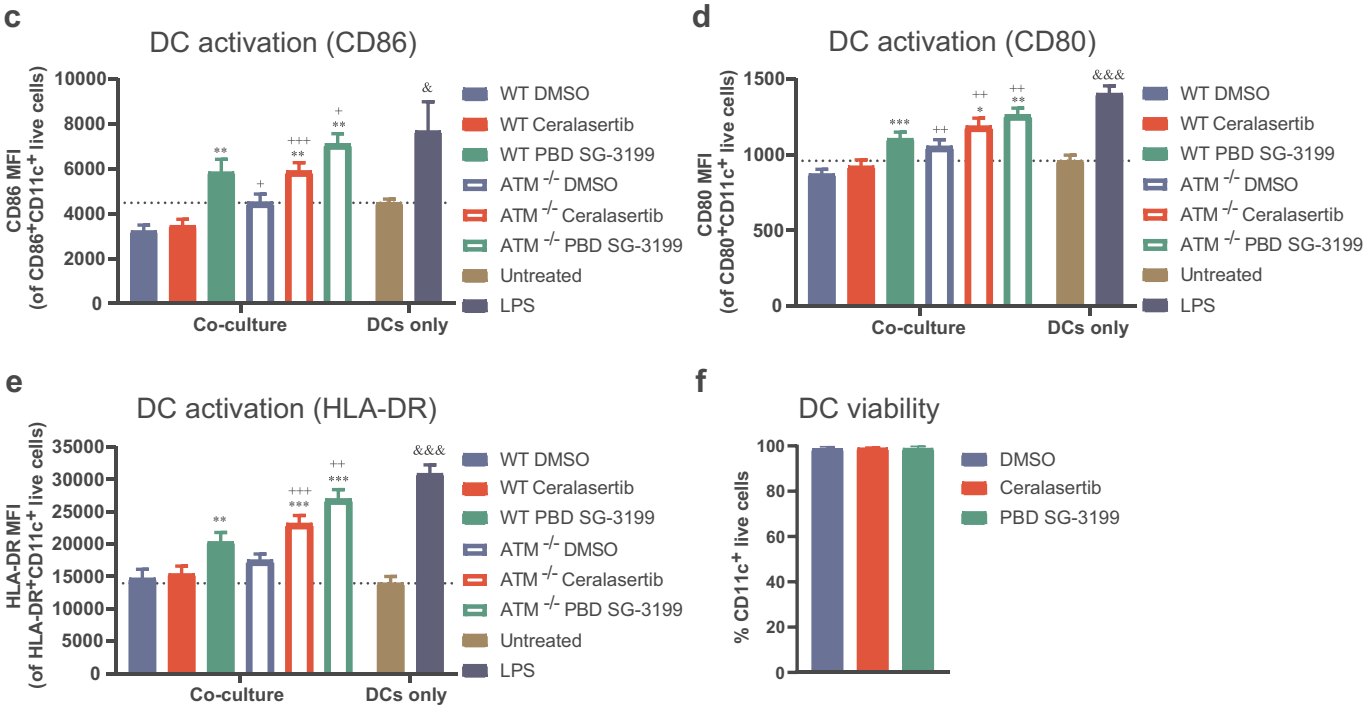

Figure 5. ATR inhibition and DNA damage in ATM-deficient tumor cells induce enhanced efferocytosis of tumor cells and DC activation.
(a-e) FaDu WT and FaDu ATM $^{-/-}$ cells were labeled with CellTrace violet and treated with ceralasertib (1μM) or PBD SG-3199 (40 pM) for 48 hours followed by co-culture with primary human dendritic cells (DCs) (20:1 ratio tumor cells: DCs). DCs stimulated with LPS (10ng/ml) for 24 hours or unstimulated were used as positive and negative controls, respectively. (a) Schematic representation of the co-culture assay. (b-e) Flow cytometric analysis of tumor cell efferocytosis (% CellTrace violet^{+}/CD11c^{+} cells within CD11c^{+} live single cells) (b) and DC activation (median fluorescence intensity (MFI) of CD86, CD80 and HLA-DR within CD86^{+}CD11c^{+}, CD80^{+}CD11c^{+} and HLA-DR^{+}CD11c^{+} live single cells, respectively) (c-e). Data shown as mean + SEM of one representative experiment out of three independent experiments performed. Each experiment was performed with three or four donors. Statistical analysis by paired t-test ($p<.05$ *, $p<.01$ **, $p<.001$ *** comparing treatment vs DMSO control in each genotype; $p<.05$ +, $p<.01$ ++, $p<.001$ +++ comparing each treatment group in WT vs ATM $^{-/-}$ cells; $p<.05$ &, $p<.01$ &&, $p<.001$ &&& comparing untreated and LPS-stimulated dendritic cells monoculture control). See also Supplementary Figure S7. (f) Dendritic cells were treated with ceralasertib (1μM) or PBD SG-3199 (40 pM) for 48 hours and DC viability was analyzed by flow cytometry (% of blue dead^{-}/CD11c^{+} live single cells).

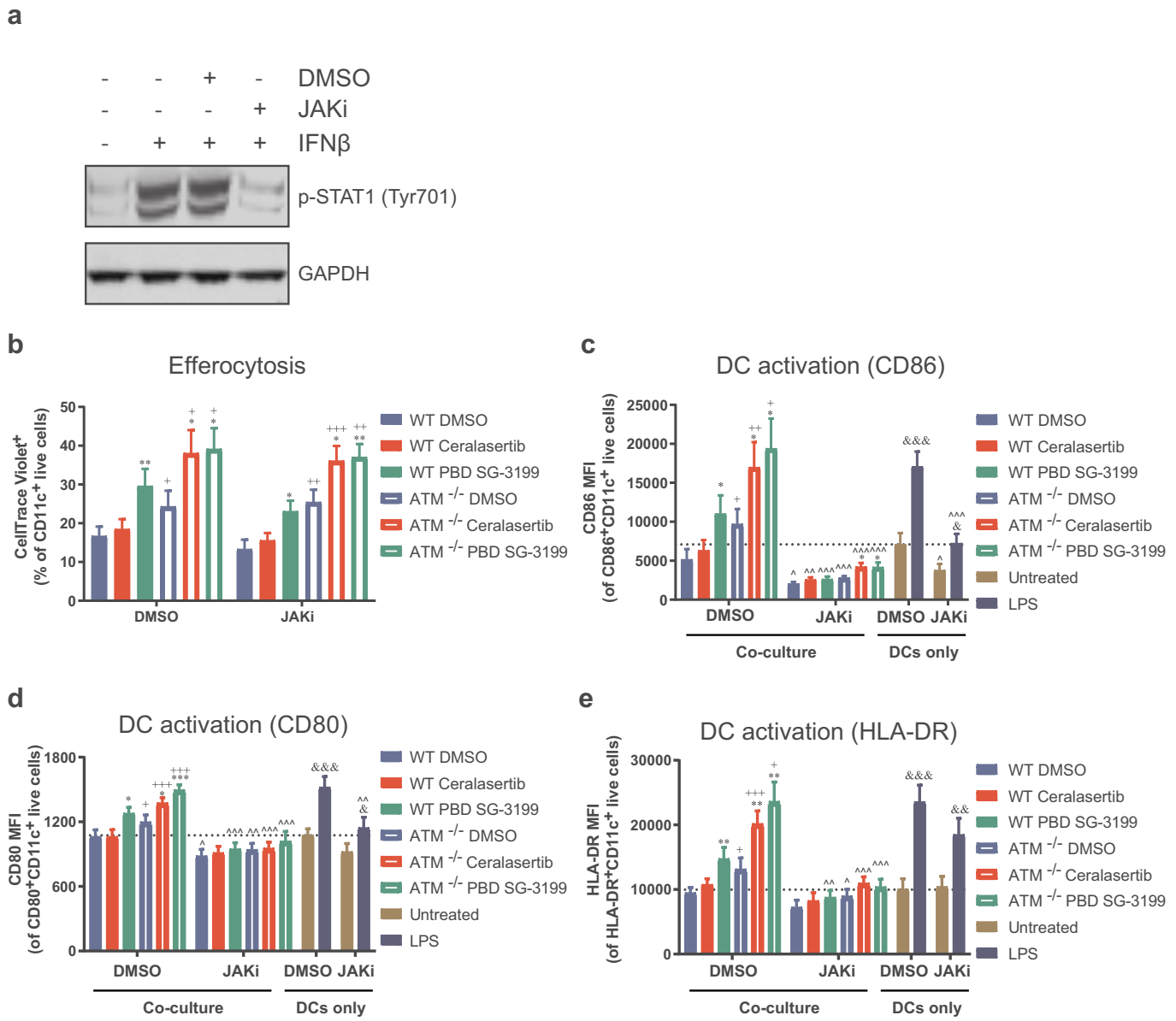

Figure 6. Inhibition of canonical JAK-STAT signaling pathway prevents activation of dendritic cells by ceralasertib or PBD SG-3199-treated tumor cells.
(a) DCs were treated with the JAK1/2 inhibitor (JAKi) INCB018424 ruxolitinib (1μM) or DMSO for one hour followed by recombinant human IFNβ (300U/ml) for 15 minutes. Cell lysates were immunoblotted with antibodies to the indicated proteins. (b-e) FaDu WT and FaDu ATM $^{-/-}$ cells labeled with CellTrace violet were treated with ceralasertib (1μM) or PBD SG-3199 (40 pM) for 48hours followed by co-culture with DCs (20:1 ratio tumor cells: DCs) in the presence of JAK1/2 inhibitor (1μM) or DMSO. DCs stimulated with LPS (10 ng/ml) for 24 hours or unstimulated used as positive and negative controls, respectively. Flow cytometric analysis of tumor cell efferocytosis (% CellTrace violet^{+}/ CD11c^{+} cells within CD11c^{+} live single cells) (b) and DC activation (median fluorescence intensity (MFI) of CD86, CD80 and HLA-DR within CD86^{+}CD11c^{+}, CD80^{+}CD11c^{+} and HLA-DR^{+}CD11c^{+} live single cells, respectively) (c-e). Data shown as mean + SEM of one representative experiment out of three independent experiments performed. Each experiment was performed with three or four donors. Statistical analysis by paired t-test (p<.05 *, p<.01 **, p<.001 *** comparing treatment vs DMSO control in each genotype; p<.05 +, p<.01 ++, p<.001 +++ comparing each treatment group in WT vs ATM −/− cells; p<.05 &, p<.01 &&, p<.001 &&& comparing untreated and LPS-stimulated dendritic cells monoculture control; p<.05 ^, p<.01 ^^, p<.001 ^^^ comparing JAKi treated vs DMSO control treated for each treatment and genotype in co-cultures and DCs monoculture).

we used the commercially available THP-1 cells. THP-1 cells are not sensitive to ceralasertib **(Figure S8)**, therefore we continued the studies with PBD SG-3199 and IR treatments. PBD SG-3199 (Figure 7a) and IR treatment **(Figure S9A)** induced more cell death in TREX1 $^{-/-}$ cells compared to WT cells. TREX1 depletion also increased basal cell death (Figures 7a **and S9A)**. Moreover, treatment of TREX1 $^{-/-}$ tumor cells with IR **(Figure S9B)** or PBD SG-3199 (Figure 7b) resulted in increased IFNβ mRNA expression as compared to WT cells. Notably, TREX1 depletion did not result in higher IFNβ mRNA expression in untreated cells (Figure 7b **and S9B)**. When co-cultured with DCs, we observed that both WT and TREX1 $^{-/-}$ cells induced efferocytosis and DC activation when treated with IR or PBD SG-3199 (**Figure S9C–D and** 7c–f). TREX1 deficiency increased efferocytosis and DC activation in response to both IR and PBD SG-3199 **(Figure S9C–D and** 7c–f). In addition, untreated TREX1 $^{-/-}$ tumor cells induced higher levels of DC activation but not efferocytosis, suggesting that loss of TREX1 increases cytoplasmic DNA levels **(Figure S9C–D and** 7c–f).

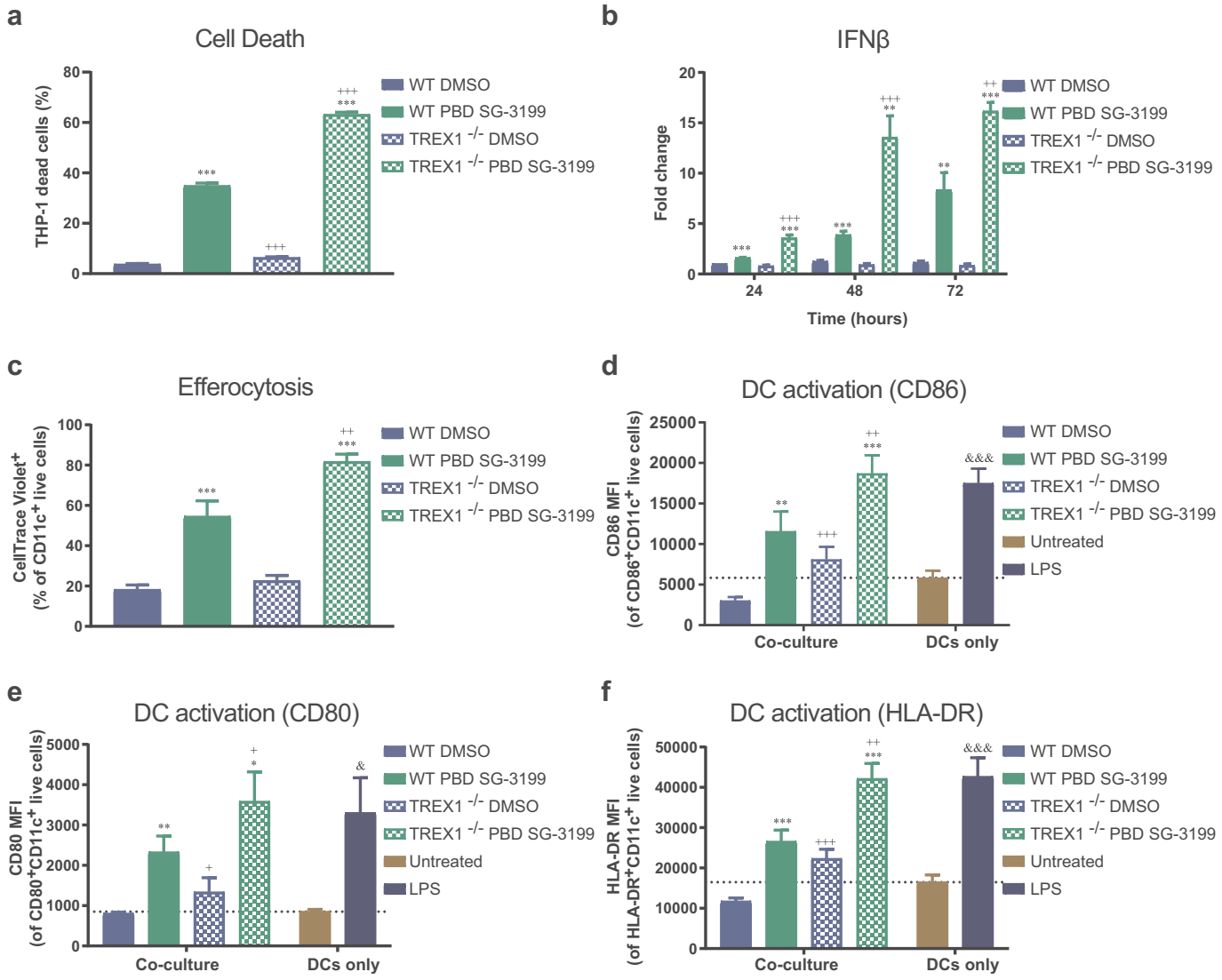

Figure 7. Enhanced cell death, IFNβ mRNA induction and increased efferocytosis and DC activation by PBD SG-3199 treated TREX1-deficient tumor cells. (a) THP-1 WT and THP-1 TREX1 $^{-/-}$ cells treated for 48 hours with PBD SG-3199 (400 pM) and cell death analysis was performed by flow cytometry. Data are shown as mean + SEM of percentage of blue dead^{+} cells of the single cell population from three independent experiments. Each experiment was performed in duplicate. (b) IFNβ mRNA expression of THP-1 WT and THP-1 TREX1 $^{-/-}$ cells treated for the times indicated in the figures with PBD SG-3199 (400 pM) analyzed by RT-qPCR. Data normalized to GAPDH shown as mean + SEM fold increase relative to THP-1 WT DMSO-treated cells from two independent experiments. Each experiment was performed in triplicate. (a-b) Statistical testing by t-test (p<.05 *, p<.01 **, p<.001 *** comparing treatment vs DMSO control in each genotype; p<.05 +, p<.01 ++, p<.001 +++ comparing each treatment group in WT vs TREX1 $^{-/-}$ cells). (c-f) THP-1 WT and THP-1 TREX1 $^{-/-}$ cells were labeled with CellTrace violet and treated with PBD SG-3199 (400 pM) for 24 hours followed by co-culture with DCs (20:1 ratio tumor cells: DCs) for 24 hours. DCs stimulated with LPS (10 ng/ml) for 24 hours or unstimulated used as positive and negative controls, respectively. Flow cytometric analysis of tumor cell efferocytosis (% CellTrace violet^{+}/ CD11c^{+} cells within CD11c^{+} live cells) (c) and DC activation (median fluorescence intensity (MFI) of CD86, CD80 and HLA-DR within CD86^{+}CD11c^{+}, CD80^{+}CD11c^{+} and HLA-DR^{+}CD11c^{+} live single cells, respectively) (d-f). Data shown as mean + SEM from three independent experiments. Each experiment was performed with four to six donors. Statistical analysis by paired t-test (p<.05 *, p<.01 **, p<.001 *** comparing treatment vs DMSO control in each genotype; p<.05 +, p<.01 ++, p<.001 +++ comparing each treatment group in WT vs TREX1 $^{-/-}$ cells; p<.05 &, p<.01 &&, p<.001 &&& comparing untreated and LPS-stimulated dendritic cells monoculture control). See also Supplementary Figure S9.

STING deficiency in tumor cells does not prevent DC activation by PBD SG-3199-treated tumor cells

We have shown that ceralasertib or PBD SG-3199 treatment in sensitive tumor cell lines induced a STING-dependent type-I IFN signature and a canonical JAK-STAT signaling dependent activation of DCs. We have also shown that loss of TREX1 in THP-1 tumor cells increased tumor cell-derived type-I IFN mRNA induction and the activation of DCs in response to PBD SG-3199 treatment. These results suggest that the accumulation of cytosolic DNA in the treated tumor cells and subsequent activation of the STING pathway is responsible for the observed DC activation. STING deficiency did not modulate the induction of cell death in response to PBD SG-3199, however there was a baseline increase in cell death in STING $^{-/-}$ cells when compared to WT cells (Figure 8a). To determine if STING pathway competence in tumor cells is required for their efferocytosis by DCs and DC activation following treatment with PBD SG-3199, we co-cultured DCs with PBD SG-3199-treated THP-1 WT or THP-1 STING $^{-/-}$ cells. Untreated THP-1 STING $^{-/-}$ cells induced higher levels of efferocytosis and DC activation than THP-1 WT cells (Figure 8b–e). However, treatment of WT and STING $^{-/-}$ THP-1 cells

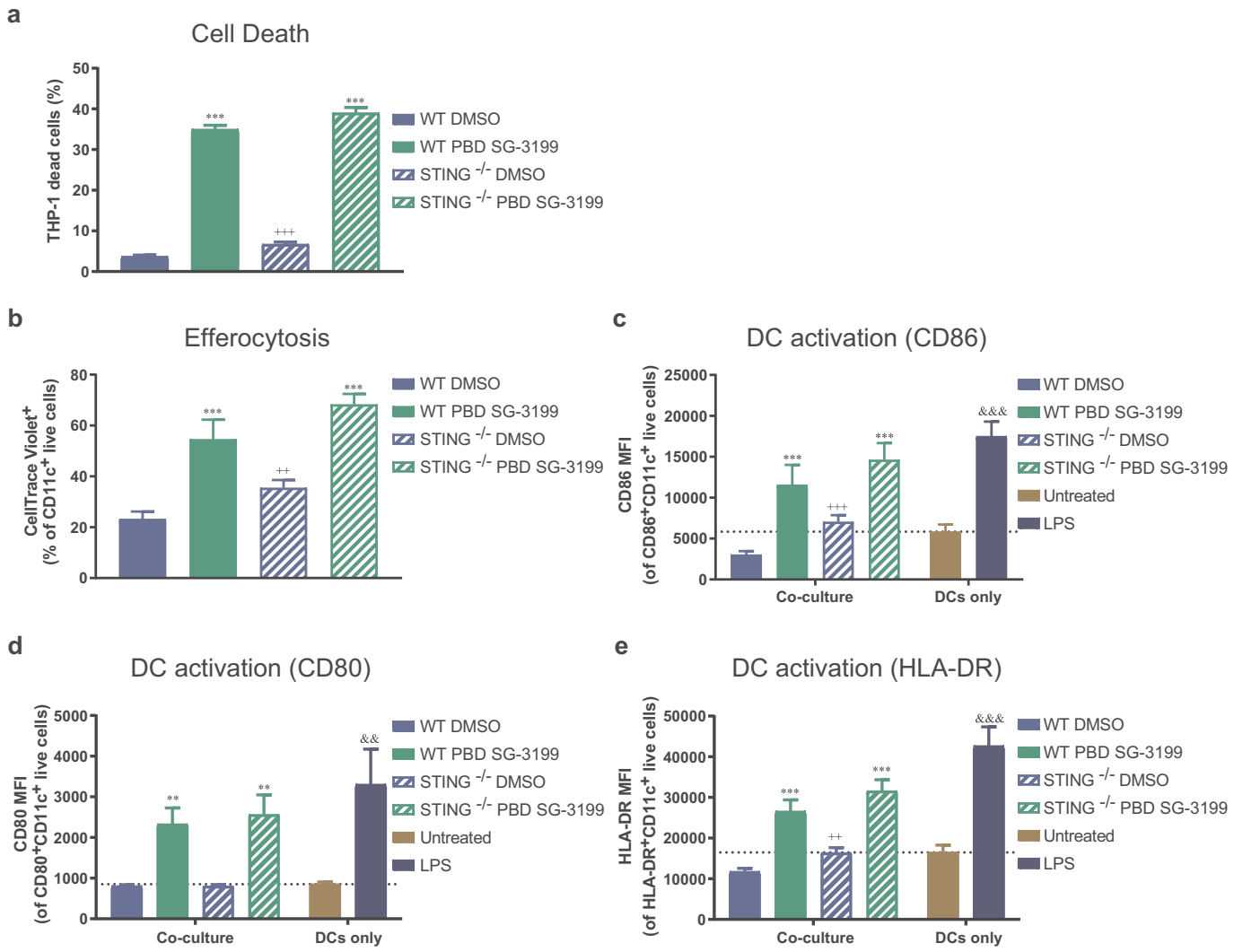

Figure 8. STING deficiency in tumor cells does not modulate cell death, efferocytosis or prevent DC activation by PBD SG3199-treated tumor cells.
(a) THP-1 WT and THP-1 STING $^{-/-}$ cells treated for 48 hours with PBD SG-3199 (400 pM) and cell death analysis was performed by flow cytometry. Data are shown as mean + SEM of percentage of blue dead^{+} cells of the single cell population from three independent experiments. Each experiment was performed in duplicate. Statistical testing by t-test ($p < .05$ *, $p < .01$ **, $p < .001$ *** comparing treatment vs DMSO control in each genotype; $p < .05$ +, $p < .01$ ++, $p < .001$ +++ comparing each treatment group in WT vs STING $^{-/-}$ cells. (b-e) THP-1 WT and THP-1 STING $^{-/-}$ cells were labeled with CellTrace violet and treated with PBD SG-3199 (400 pM) for 24 hours followed by co-culture with DCs (20:1 ratio tumor cells: DCs) for 24 hours. Flow cytometric analysis of tumor cell efferocytosis (% CellTrace violet^{+}/ CD11c^{+} cells within CD11c^{+} live single cells) (b) and DC activation (median fluorescence intensity (MFI) of CD86, CD80 and HLA-DR within CD86^{+}CD11c^{+}, CD80^{+}CD11c^{+} and HLA-DR^{+}CD11c^{+} live single cells, respectively) (c-e). DCs stimulated with LPS (10 ng/ml) for 24 hours or unstimulated used as positive and negative controls, respectively (c-e). Data shown as mean + SEM from three independent experiments. Each experiment was performed with four to six donors. Statistical testing by paired t-test ($p < .05$ *, $p < .01$ **, $p < .001$ *** comparing treatment vs DMSO control in each genotype; $p < .05$ +, $p < .01$ ++, $p < .001$ +++ comparing each treatment group in WT vs STING $^{-/-}$ cells; $p < .05$ &, $p < .01$ &&, $p < .001$ &&& comparing untreated and LPS-stimulated dendritic cells monoculture control).

with PBD SG-3199 induced similar increases in both efferocytosis and DC activation (Figure 8b–e). These data indicate that competence in the STING pathway in tumor cells is not obligatory for efferocytosis by, and activation of, DCs.

Discussion

Activation of the immune system has been shown to be involved in the antitumor effect of cytoreductive therapies including radiotherapy[5] and certain chemotherapies such as anthracyclines.[4] Although the mechanism for this activation of the immune system is not clearly defined, it is thought that the direct effect these therapies have on killing tumor cells releases DAMPs that serve as immunostimulatory danger signals. Several DAMPs have been identified as immunogenic, such as the ecto-expression of calreticulin, release of extracellular ATP, heat shock proteins, high mobility group box 1 (HMGB1) proteins as well as the induction of type-I IFN (reviewed in Ref. [28,44]. Indeed, the induction of immunogenic cell death by some chemotherapies and radiotherapy may be critical for their therapeutic efficacy.[10]

In this study, we sought to elucidate the effect of targeting the DNA damage response machinery with the ATR inhibitor ceralasertib[20] or inducing DNA damage with PBD SG-3199 on the ability of tumor cells to elicit activation of the innate immune system against the damaged tumor. ATR inhibition has previously been shown to cause synthetic lethality in ATM-deficient cells[2] and we have shown here that this induces an

enhanced cell cycle arrest and DNA damage as well as early apoptosis and cell death and inhibition of proliferation in ATM-deficient cells in comparison with WT cells. Moreover, we have demonstrated that ceralasertib induces an enhanced type-I IFN signature in ATM-deficient tumor cells. It has been reported that ATM deficiency also increases the sensitivity of tumor cells to DNA damaging agents. For example, defects in the DNA damage repair protein ERCC1 have been shown to increase sensitivity to the DNA damaging agent PBD SG-3199.[3] Here, we have demonstrated that ATM deficiency enhances sensitivity of the tumor cells to PBD SG-3199 with an increased DNA damage, early apoptosis, cell death and inhibition of proliferation. Moreover, ATM deficiency also increases the induction of type-I IFN in response to DNA damage induced by IR and induces a more rapid type-I IFN response to the DNA damaging agent PBD SG-3199. Furthermore, ATM deficiency also increases basal levels of type-I IFN expression. These data correlate with previous studies where it was found that loss of function mutations of ATM in humans that result in Ataxia Telangiectasia (AT), a cancer-prone inflammatory neurodegenerative disease with an increase in sensitivity to radiation, induce spontaneous release of type-IFN.[35]

The activation of the STING pathway has been shown to play a critical role for the activation of the innate immune system in response to DNA damage induction in the tumor (reviewed in Ref. [29]). For example, it has been shown that DNA damage in tumor cells deficient in BRCA1 induces a type-I IFN signaling by activation of the STING pathway.[45] Moreover, the treatment of BRCA1-deficient tumors with the PARP1 inhibitor olaparib induces STING-dependent antitumor immunity.[46] Here, we have shown that STING deficiency blocks the induction of IFNβ in response to the ATR inhibitor ceralasertib, and by the DNA crosslinker PBD SG-3199. cGAS[15] and IFI16[47] are two DNA sensors that have been reported to induce STING activation. Although, it has been proposed that the activation of STING by DNA damage induced by etoposide in human keratocytes is not cGAS dependent but IFI16 dependent instead,[33] here we have shown that cGAS silencing also abolished type-IFN induction by ceralasertib and PBD SG-3199 in FaDu tumor cells, indicating that in this context cGAS is the key DNA sensor that induces STING activation. These data correlate with other studies which have shown that DNA damage is detected by cGAS. DNA damage in the nucleus generates genomic instability leading to the accumulation of nuclear DNA in the cytosol in the form of micronuclei. cGAS co-localizes with micronuclei formed after DNA damage[25] and induces the activation of type-I IFN by cGAS-STING pathway.[26] Here, we have demonstrated that ceralasertib and PBD SG-3199 induce micronuclei formation in both WT and ATM-deficient tumor cells but it is enhanced in ATM-deficient cells. This may explain the induction of type-I IFN by ceralasertib and PBD SG-3199 in these cells, but other mechanisms cannot be excluded. In this context, it has been published that the cleavage of genomic DNA by the endonuclease MUS81 during the response to replication stress induces the accumulation of dsDNA in the cytosol of cancer cells, STING-dependent type-I IFN induction, immune recognition of the tumor cells and immune rejection.[48] In conclusion, different forms of cytosolic DNA can be accumulated after DNA damage induction or targeting DNA damage response proteins activating a STING-dependent type-I IFN signature in the tumor cells.

Type-I IFN is essential for the induction of an adaptive antitumor immunity and tumor regression in response to DNA damage by IR.[38] Moreover, the induction of type-IFN by radiation and consequent cross-priming of $CD8^+$ T cells by dendritic cells is dependent on cGAS-STING signaling.[17] Furthermore, deletion of the type-I IFN receptor on dendritic cells prevents the antitumor activity of radiation.[18] In summary, these data suggest that dendritic cells are required for the antitumor efficacy of radiation by inducing adaptive immune responses. Our data shows that the treatment of sensitive tumor cells with ceralasertib, PBD SG-3199 or IR induces the efferocytosis of the tumor cells by human primary dendritic cells and dendritic cell activation, boosted in ATM-deficient tumor cells. The inhibition of the canonical JAK-STAT signaling pathway downstream of type-I IFN by ruxolitinib completely abolishes dendritic cell activation in response to treated tumor cells. These data further confirm that the activation of dendritic cells in response to tumor cells treated with DNA damage targeting therapies is type-I IFN dependent. We have also shown that unlike tumor cells, DC viability is not affected by ceralasertib or PBD SG-3199 treatment *in vitro*, possibly because DCs do not proliferate.[49] However, a limitation of the present study is that we have not investigated the possible direct effects that systemic administration of ceralasertib or PBD SG-3199 treatment may have on DCs or other immune cells *in vivo* that may affect antitumor immunity.

Deregulation of STING expression or STING signaling correlates with increased tumorigenesis and poor prognosis.[30,31] Here, we have shown that the activation of dendritic cells in response to PBD SG-3199-treated THP-1 tumor cells is not affected by STING deficiency in the tumor cells, indicating that the activation of STING in the tumor cells is not needed for the induction of dendritic cell activation in response to PBD-treated tumor cells. Recent publications have proposed that tumor-infiltrating dendritic cells are the main cell type involved in STING-mediated type-I IFN production. In response to radiation, tumor-derived DNA can be detected in the cytosol of APCs and drive the activation of dendritic cells.[17] Cell to cell contact is essential for the transactivation of the STING pathway in dendritic cells and for antitumor immunity.[50] These data suggest that tumor-derived DNA activates the STING pathway in dendritic cells. However, we cannot exclude the possibility that the initial production of type-I IFN by the tumor cells has a role in antitumor immunity *in vivo*. Regarding this, it has been reported that the induction of type-I IFN by the activation of the cGAS-STING pathway in cancer cells is required to attract dendritic cells and subsequent cross-presentation of antigens to T cells.[43] The precise mechanism by which endogenous tumor DNA can access the cytosol of dendritic cells to activate the cGAS-STING pathway in response to ceralasertib or PBD SG-3199 remains unclear. We have shown that the treatment of sensitive tumor cell lines with ceralasertib and PBD SG-3199 induces the efferocytosis of treated tumor cells by dendritic cells. This may be a mechanism by which tumor-derived DNA gets into the cytosol of dendritic cells. Exosomes have also been proposed as a mechanism by which tumor-derived dsDNA from irradiated tumor cells transfer to dendritic cells inducing type-I IFN.[51]

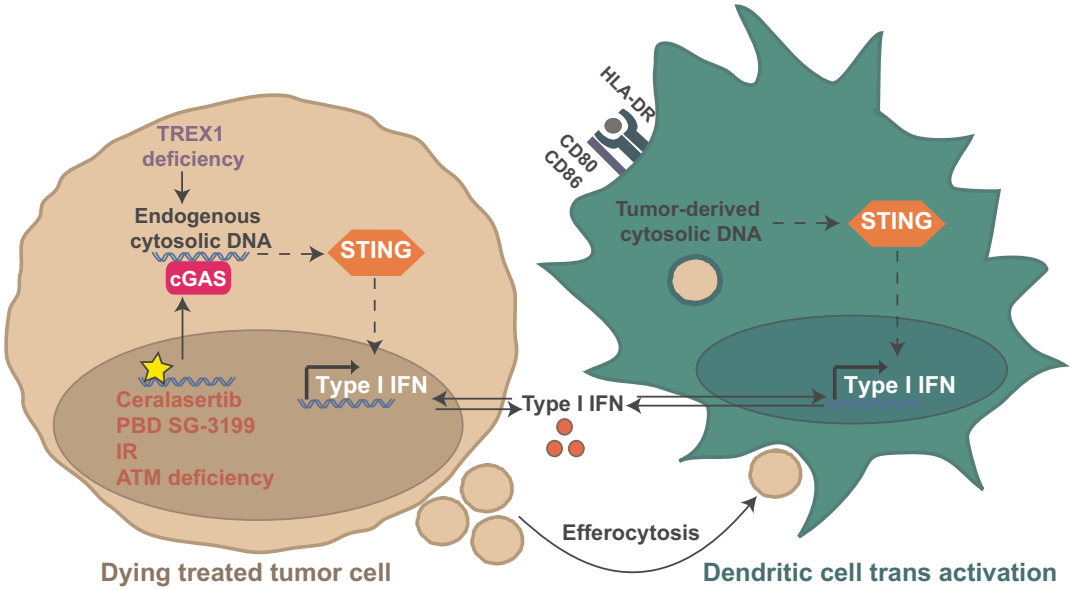

Figure 9. Proposed mechanism of action.
The treatment of sensitive tumor cells with the DNA damage response inhibitor ceralasertib or with the DNA damaging agents PBD SG-3199 or IR induce a cGAS-STING-dependent type-I IFN signature enhanced in ATM-deficient tumor cells. Dying treated tumor cells are efferocytosed by DC and induce type-I IFN-dependent DC activation. The activation of dendritic cells is not prevented by STING deficiency in tumor cells, suggesting that tumor-derived DNA transactivate STING pathway in DCs. Moreover, TREX1 depletion in tumor cells also increased type-I IFN expression by tumor cells and DC activation in response to treated tumor cells.

Further experiments would be required to fully delineate the mechanism by which tumor DNA from ceralasertib or PBD SG-3199 treated cells may get access to the cytosol of DCs. STING activation is tightly regulated by the exonuclease TREX1. It has been proposed that whereas low doses of radiotherapy are effective at inducing antitumor responses, high doses of radiotherapy may increase TREX1 expression in tumor cells leading to degradation of cytosolic DNA in the tumor and attenuation of type-I IFN dependent dendritic cell activation and cross-presentation to $CD8^+$ T cells.[43] In contrast, in this study we show that high doses of radiation are able to induce type-I IFN in both FaDu and THP-1 tumor cells, indicating that the ability of different doses of radiation to induce type-I IFN response may be tumor cell dependent. Nevertheless, TREX1 deficiency within the tumor cells further increased the induction of type-I IFN and boosted dendritic cell activation in response to co-culture with tumor cells treated with the DNA damaging agents IR or PBD SG-3199. The increased activation of dendritic cells by treated TREX1-deficient tumor cells could also be due, at least partially, to increased tumor cell death and efferocytosis in treated TREX1 $^{-/-}$ tumor cells. In general, these data suggest that tumor-derived DNA can extrinsically transactivate dendritic cells.

We have shown that ATM deficiency not only increases the intrinsic sensitivity of tumor cells to DNA damaging agents and to synthetic lethality when combined with ATR inhibition, but that these treatments also increase the immunogenicity of these cellular insults via STING-dependent production of type-I IFN by dendritic cells. Moreover, we show that TREX1 is an important rheostat for controlling this immunogenicity via the degradation of cytosolic DNA (diagram in Figure 9). Taken together these data offer new insights into how combinations of cytotoxic chemotherapy payloads, such as those used in ADC, can be combined with inhibitors of the DNA-damage response to not only enhance direct cytotoxicity but also immune recognition and priming.

Disclosure statement

All authors were employees at and stock holders of AstraZeneca at the time of the study.

Funding

The author(s) reported there is no funding associated with the work featured in this article.

Data availability

The data that support the findings of this study are available from the corresponding author SJD, upon reasonable request.

References

1. O'Connor MJ. Targeting the DNA Damage Response in Cancer. Mol Cell. 2015;60(4):547–560. doi:10.1016/j.molcel.2015.10.040.
2. Reaper PM, et al. Selective killing of ATM- or p53-deficient cancer cells through inhibition of ATR. Nat Chem Biol. 2011;7(7):428–430. doi:10.1038/nchembio.573.
3. Hartley JA, et al. Pre-clinical pharmacology and mechanism of action of SG3199, the pyrrolobenzodiazepine (PBD) dimer warhead component of antibody-drug conjugate (ADC) payload tesirine. Sci Rep. 2018;8(1):10479. doi:10.1038/s41598-018-28533-4.
4. Casares N, et al. Caspase-dependent immunogenicity of doxorubicin-induced tumor cell death. J Exp Med. 2005;202(12):1691–1701. doi:10.1084/jem.20050915.
5. Obeid M, et al. Calreticulin exposure is required for the immunogenicity of gamma-irradiation and UVC light-induced apoptosis. Cell Death Differ. 2007;14(10):1848–1850. doi:10.1038/sj.cdd.4402201.

6. Gallo PM, Gallucci S. The dendritic cell response to classic, emerging, and homeostatic danger signals. Implications for autoimmunity. Vol. 4, Front Immunol; 2013. p. 138.
7. Boada-Romero E, et al. The clearance of dead cells by efferocytosis. Nat Rev Mol Cell Biol. 2020;21(7):398–414. doi:10.1038/s41580-020-0232-1.
8. Ghiringhelli F, et al. Activation of the NLRP3 inflammasome in dendritic cells induces IL-1beta-dependent adaptive immunity against tumors. Nat Med. 2009;15(10):1170–1178. doi:10.1038/nm.2028.
9. Obeid M, et al. Calreticulin exposure dictates the immunogenicity of cancer cell death. Nat Med. 2007;13(1):54–61. doi:10.1038/nm1523.
10. Apetoh L, et al. Toll-like receptor 4-dependent contribution of the immune system to anticancer chemotherapy and radiotherapy. Nat Med. 2007;13(9):1050–1059. doi:10.1038/nm1622.
11. Kwon J, Bakhoum SF. The Cytosolic DNA-Sensing cGAS-STING Pathway in Cancer. Cancer Discov. 2020;10(1):26–39. doi:10.1158/2159-8290.CD-19-0761.
12. Ishikawa H, Barber GN. STING is an endoplasmic reticulum adaptor that facilitates innate immune signalling. Nature. 2008;455(7213):674–678. doi:10.1038/nature07317.
13. Ishikawa H, Ma Z, Barber GN. STING regulates intracellular DNA-mediated, type I interferon-dependent innate immunity. Nature. 2009;461(7265):788–792. doi:10.1038/nature08476.
14. Sun L, et al. Cyclic GMP-AMP synthase is a cytosolic DNA sensor that activates the type I interferon pathway. Science. 2013;339(6121):786–791. doi:10.1126/science.1232458.
15. Wu J, et al. Cyclic GMP-AMP is an endogenous second messenger in innate immune signaling by cytosolic DNA. Science. 2013;339(6121):826–830. doi:10.1126/science.1229963.
16. Burdette DL, et al. STING is a direct innate immune sensor of cyclic di-GMP. Nature. 2011;478(7370):515–518. doi:10.1038/nature10429.
17. Woo SR, et al. STING-dependent cytosolic DNA sensing mediates innate immune recognition of immunogenic tumors. Immunity. 2014;41(5):830–842. doi:10.1016/j.immuni.2014.10.017.
18. Deng L, et al. STING-Dependent Cytosolic DNA Sensing Promotes Radiation-Induced Type I Interferon-Dependent Antitumor Immunity in Immunogenic Tumors. Immunity. 2014;41(5):843–852. doi:10.1016/j.immuni.2014.10.019.
19. Corrales L, et al. Direct Activation of STING in the Tumor Microenvironment Leads to Potent and Systemic Tumor Regression and Immunity. Cell Rep. 2015;11(7):1018–1030. doi:10.1016/j.celrep.2015.04.031.
20. Vendetti FP, et al. The orally active and bioavailable ATR kinase inhibitor AZD6738 potentiates the anti-tumor effects of cisplatin to resolve ATM-deficient non-small cell lung cancer in vivo. Oncotarget. 2015;6(42):44289–44305. doi:10.18632/oncotarget.6247.
21. Ward TA, McHugh PJ, Durant ST. Small molecule inhibitors uncover synthetic genetic interactions of human flap endonuclease 1 (FEN1) with DNA damage response genes. PLoS One. 2017;12(6):e0179278. doi:10.1371/journal.pone.0179278.
22. Pike KG, et al. *The Identification of Potent, Selective, and Orally Available Inhibitors of Ataxia Telangiectasia Mutated (ATM) Kinase: the Discovery of AZD0156 (8-{6-[3-(Dimethylamino)propoxy]pyridin-3-yl}-3-methyl-1-(tetrahydro-2 H-pyran-4-yl)-1,3-dihydro-2 H-imidazo[4,5-c]quinolin-2-one)*. J Med Chem. 2018;61(9):3823–3841. doi:10.1021/acs.jmedchem.7b01896.
23. Lloyd RL, et al. Combined PARP and ATR inhibition potentiates genome instability and cell death in ATM-deficient cancer cells. Oncogene. 2020;39(25):4869–4883. doi:10.1038/s41388-020-1328-y.
24. Min A, et al. AZD6738, A Novel Oral Inhibitor of ATR, Induces Synthetic Lethality with ATM Deficiency in Gastric Cancer Cells. Mol Cancer Ther. 2017;16(4):566–577. doi:10.1158/1535-7163.MCT-16-0378.
25. Mackenzie KJ, et al. cGAS surveillance of micronuclei links genome instability to innate immunity. Nature. 2017;548(7668):461–465. doi:10.1038/nature23449.
26. Harding SM, et al. Mitotic progression following DNA damage enables pattern recognition within micronuclei. Nature. 2017;548(7668):466–470. doi:10.1038/nature23470.
27. Dillon MT, et al. Radiosensitization by the ATR Inhibitor AZD6738 through Generation of Acentric Micronuclei. Mol Cancer Ther. 2017;16(1):25–34. doi:10.1158/1535-7163.MCT-16-0239.
28. Kroemer G, et al. Immunogenic cell death in cancer therapy. Annu Rev Immunol. 2013;31:51–72. doi:10.1146/annurev-immunol-032712-100008.
29. Li T, Chen ZJ. The cGAS-cGAMP-STING pathway connects DNA damage to inflammation, senescence, and cancer. J Exp Med. 2018;215(5):1287–1299. doi:10.1084/jem.20180139.
30. Song S, et al. Decreased expression of STING predicts poor prognosis in patients with gastric cancer. Sci Rep. 2017;7:39858. doi:10.1038/srep39858.
31. Xia T, et al. Deregulation of STING Signaling in Colorectal Carcinoma Constrains DNA Damage Responses and Correlates With Tumorigenesis. Cell Rep. 2016;14(2):282–297. doi:10.1016/j.celrep.2015.12.029.
32. Zhang X, et al. Cyclic GMP-AMP containing mixed phosphodiester linkages is an endogenous high-affinity ligand for STING. Mol Cell. 2013;51(2):226–235. doi:10.1016/j.molcel.2013.05.022.
33. Dunphy G, et al. Non-canonical Activation of the DNA Sensing Adaptor STING by ATM and IFI16 Mediates NF-kappaB Signaling after Nuclear DNA Damage. Mol Cell. 2018;71(5):745–760 e5. doi:10.1016/j.molcel.2018.07.034.
34. Riches LC, et al. Pharmacology of the ATM Inhibitor AZD0156: potentiation of Irradiation and Olaparib Responses Preclinically. Mol Cancer Ther. 2020;19(1):13–25. doi:10.1158/1535-7163.MCT-18-1394.
35. Hartlova A, et al. DNA damage primes the type I interferon system via the cytosolic DNA sensor STING to promote anti-microbial innate immunity. Immunity. 2015;42(2):332–343. doi:10.1016/j.immuni.2015.01.012.
36. McLellan AD, et al. Activation of human peripheral blood dendritic cells induces the CD86 co-stimulatory molecule. Eur J Immunol. 1995;25(7):2064–2068. doi:10.1002/eji.1830250739.
37. Banchereau J, et al. Immunobiology of dendritic cells. Annu Rev Immunol. 2000;18:767–811. doi:10.1146/annurev.immunol.18.1.767.
38. Burnette BC, et al. The efficacy of radiotherapy relies upon induction of type I interferon-dependent innate and adaptive immunity. Cancer Res. 2011;71(7):2488–2496. doi:10.1158/0008-5472.CAN-10-2820.
39. Platanias LC. Mechanisms of type-I- and type-II-interferon-mediated signalling. Nat Rev Immunol. 2005;5(5):375–386. doi:10.1038/nri1604.
40. Quintas-Cardama A, et al. Preclinical characterization of the selective JAK1/2 inhibitor INCB018424: therapeutic implications for the treatment of myeloproliferative neoplasms. Blood. 2010;115(15):3109–3117. doi:10.1182/blood-2009-04-214957.
41. Heine A, et al. The JAK-inhibitor ruxolitinib impairs dendritic cell function in vitro and in vivo. Blood. 2013;122(7):1192–1202. doi:10.1182/blood-2013-03-484642.
42. Ahn J, Ruiz P, Barber GN. Intrinsic self-DNA triggers inflammatory disease dependent on STING. J Immunol. 2014;193(9):4634–4642. doi:10.4049/jimmunol.1401337.
43. Vanpouille-Box C, et al. DNA exonuclease Trex1 regulates radiotherapy-induced tumour immunogenicity. Vol. 8. Nat Commun; 2017. p. 15618.
44. Green DR, et al. Immunogenic and tolerogenic cell death. Nat Rev Immunol. 2009;9(5):353–363. doi:10.1038/nri2545.
45. Parkes EE, et al. Activation of STING-Dependent Innate Immune Signaling By S-Phase-Specific DNA Damage in Breast Cancer. J Natl Cancer Inst. 2017;109(1). doi:10.1093/jnci/djw199.

46. Ding L, et al. PARP Inhibition Elicits STING-Dependent Antitumor Immunity in Brca1-Deficient Ovarian Cancer. Cell Rep. 2018;25(11):2972–2980 e5. doi:10.1016/j.celrep.2018.11.054.
47. Unterholzner L, et al. IFI16 is an innate immune sensor for intracellular DNA. Nat Immunol. 2010;11(11):997–1004. doi:10.1038/ni.1932.
48. Ho SS, et al. The DNA Structure-Specific Endonuclease MUS81 Mediates DNA Sensor STING-Dependent Host Rejection of Prostate Cancer Cells. Immunity. 2016;44(5):1177–1189. doi:10.1016/j.immuni.2016.04.010.
49. Cavanagh LL, et al. Proliferation in monocyte-derived dendritic cell cultures is caused by progenitor cells capable of myeloid differentiation. Blood. 1998;92(5):1598–1607. doi:10.1182/blood.V92.5.1598.
50. Ahn J, et al. Extrinsic Phagocyte-Dependent STING Signaling Dictates the Immunogenicity of Dying Cells. Cancer Cell. 2018;33(5):862–873 e5. doi:10.1016/j.ccell.2018.03.027.
51. Diamond JM, et al. Exosomes Shuttle TREX1-Sensitive IFN-Stimulatory dsDNA from Irradiated Cancer Cells to DCs. Cancer Immunol Res. 2018;6(8):910–920. doi:10.1158/2326-6066.CIR-17-0581.